Nafta-Gaz 2025, no. 10, pp. 690–702, DOI: 10.18668/NG.2025.10.05

Investigation of the effect of a new composition on the demulsification of Umbaki oil and mathematical modeling of the results

Badanie wpływu nowej kompozycji na deemulgację ropy Umbaki oraz modelowanie matematyczne wyników

Guseyn R. Gurbanov, Aysel V. Gasimzade

Azerbaijan State Oil and Industry University

ABSTRACT: The present article investigates the demulsification process of highly stable water-oil emulsion from the Umbaki field, one of the heavy oil-producing sites operated by SOCAR in Azerbaijan. The study employed both physical (temperature effect) and physicochemical methods using ND-12 (Azerbaijan) and Dissolvan-4411 (Germany) demulsifiers, along with new compositions developed from these reagents. Emulsions were evaluated through bottle tests by calculating separated, residual, and ballast water contents. It was observed that certain emulsified oils can release a notable amount of water at 50–60°C without demulsifiers; however, Umbaki oil forms highly stable emulsions due to its heavy and resinous nature. Even at high demulsifier concentrations and elevated temperatures, the residual water content exceeded the threshold value (0.5 wt.%). To overcome this, two new compositions (A-1: ND-12 + Gossypol resin + isopropanol; A-2: Dissolvan-4411 + Gossypol resin + isopropanol) were tested and compared to individual reagents. Tests covered temperature ranges of 40–60°C. Results demonstrated that the compositions significantly enhanced demulsification efficiency, enhancing phase separation even at 60°C. The A-1 composition showed the highest performance, reducing the residual water content to 0.06% and ballast water to 0.09% at 600 g/t and 60°C. Mathematical modeling was performed for A-1 to determine its dependence on temperature, reagent dosage, and time, resulting in polynomial curves and 3D response surfaces. These findings underscore the potential of tailored reagent compositions to address the challenge of breaking down highly stable emulsions in resinous heavy oils, providing practical benefits for field operations.

Key words: reagent, composition, demulsification, water-oil emulsion, optimal concentration, efficiency, modeling.

STRESZCZENIE: Niniejszy artykuł analizuje proces deemulgacji wysoce stabilnej emulsji woda-ropa z pola Umbaki, jednego z miejsc wydobycia ropy ciężkiej eksploatowanych przez firmę SOCAR w Azerbejdżanie. W badaniach zastosowano zarówno metody fizyczne (wpływ temperatury), jak i fizykochemiczne, wykorzystując deemulgatory ND-12 (Azerbejdżan) oraz Dissolvan-4411 (Niemcy), a także nowe kompozycje opracowane na bazie tych reagentów. Emulsje oceniano metodą testów butelkowych poprzez obliczanie zawartości wody oddzielonej, resztkowej i balastowej. Zaobserwowano, że niektóre emulsje woda-ropa mogą wydzielać zauważalne ilości wody w temperaturze 50–60°C bez udziału deemulgatorów; jednak ropa z Umbaki tworzy wysoce stabilne emulsje ze względu na swój ciężki i żywiczny charakter. Nawet przy wysokich stężeniach deemulgatorów i w podwyższonych temperaturach zawartość wody resztkowej przekraczała wartość graniczną (0,5% mas.). Aby temu zaradzić, przetestowano dwie nowe kompozycje (A-1: ND-12 + żywica Gossypol + izopropanol; A-2: Dissolvan-4411 + żywica Gossypol + izopropanol) i porównano je z pojedynczymi reagentami. Badania obejmowały zakres temperatur 40–60°C. Wyniki wykazały, że kompozycje znacząco zwiększyły skuteczność deemulgacji, poprawiając rozdział faz nawet w temperaturze 60°C. Kompozycja A-1 osiągnęła najwyższą skuteczność, redukując zawartość wody resztkowej do 0,06% i wody balastowej do 0,09% przy dawce 600 g/t i w temperaturze 60°C. Dla kompozycji A-1 przeprowadzono modelowanie matematyczne w celu określenia zależności od temperatury, dawki reagenta i czasu, co pozwoliło uzyskać krzywe wielomianowe oraz trójwymiarowe powierzchnie odpowiedzi. Uzyskane wyniki podkreślają potencjał dostosowanych kompozycji reagentów w rozwiązywaniu problemu rozbijania wysoce stabilnych emulsji w żywicznych ropach ciężkich, przynosząc wymierne korzyści w praktyce eksploatacyjnej.

Słowa kluczowe: reagent, kompozycja, demulgacja, emulsja woda-ropa, stężenie optymalne, efektywność, modelowanie.

Corresponding author: G.R. Gurbanov, e-mail: *huseyn.gurbanov@asoiu.edu.az*

Article contributed to the Editor: 12.11.2024. Approved for publication: 08.09.2025.

Introduction

Preparation of oil for transportation under field conditions is a highly relevant and significant issue. Several key factors influence the stability of the emulsion formed by oil and formation water (Knapik, 2020; Abdullah et al., 2021; Xia et al., 2023). These factors include the oil's component composition and the percentage of high-molecular-weight compounds such as asphaltenes and resins, the concentration of cations and anions in formation water, the reagents applied inside the well to enhance oil recovery, mechanical mixtures, and others (Bakhtizin et al., 2016; Santos et al., 2017; Girard et al., 2020). High-molecular-weight heavy components in the oil, such as asphaltenes, resins, and paraffins, are considered natural emulsifiers, especially in relation to emulsion formation (Jennings, 2005; Zhang et al., 2007; Nebogina et al., 2008; Gurbanov et al., 2024). In particular, at high percentage of asphaltenes and, consequently, resins, enhances the stability of the emulsion formed with formation water. Since asphaltene compounds form a framework around the dispersed phases of formation water, it can be noted that asphaltene-rich oils are especially prone to forming stable emulsions. Resin components further reinforce the framework created by asphaltenes, enhancing emulsion stability (Ali and Alqam, 2000; Matiyev et al., 2016; Lee and Babadagli, 2020). Although the quantity of paraffin components is less critical for stability, they act as a barrier, protecting the robust asphaltene and resin structures from external influences (Wen et al., 2016; Taylor, 2018; Iskandarov et al., 2024). Therefore, the presence of high quantities of asphaltenes, resins, and paraffins renders the resulting emulsion highly stable.

Oils with a high content of these components are classified as heavy oils, characterized by substantial density and viscosity (Bourrel and Passade-Boupat, 2018; Liu et al., 2020; Mingalev et al., 2022).

Since emulsions formed by heavy oils are both aggregately and kinetically stable, various methods for their breakdown remain highly relevant. The most favorable methods currently involve the application of temperature and a demulsifier (Jiang et al., 2018; Zhao et al., 2021). However, it is advisable that the temperature should not exceed 60°C, while minimizing both the time and quantity of demulsifier applied. The use of compositions to enhance demulsifier effectiveness at lower temperatures is among the most efficient methods worldwide (Shayan and Mirzayi, 2015; Kharisov et al., 2017; Gurbanov and Sardarova, 2022).

Preparing the composition in the correct ratio increases the demulsifier's efficiency, resulting in greater water separation (Adams, 2014; Wang et al., 2017; Gurbanov et al., 2021; Roa et al., 2021).

Research objective

The study aims to develop and investigate highly effective compositions that reduce heat and energy consumption for the demulsification of heavy oils, which are prone to forming stable water-oil emulsions.

Research methodology

One of the widely used methods to evaluate the demulsification ability of reagents and their compositions is the bottle test (static settling) method (GOST, 1991). For this, reagents or compositions are first dissolved in a solvent and then added to the pre-selected oil samples to be investigated at various concentrations. After the reagents are added, they are mixed thoroughly for 1 minute and then left in a water bath. Depending on the demulsification ability of the tested demulsifier, the amount of separated water is recorded at various time intervals. The amount of separated water (X) is calculated using the following mathematical relation:

$$X\% = \frac{w}{w_0}100\% \quad (1)$$

where:

w_0 – initial water content in the emulsion [%, *v*/*v*],

w – separated water content during demulsification [%, *v*/*v*] (GOST, 2020).

Additionally, the amount of ballast water in the oil sample after demulsification is calculated using the following empirical formula, which incorporates the amount of water separated from the emulsion and the initial water content of a 100 g oil sample at various temperatures over a two-hour period:

$$S\% = \frac{m_1 - m_2}{m_3 - m_2}100\% \quad (2)$$

where:

S – percentage of ballast water after demulsification [%],

m_1 – amount of water in the oil before demulsification [%],

m_2 – amount of water separated from the oil during demulsification [%],

m_3 – amount of the oil sample [%] (Gurbanov and Gasimzade, 2022).

The amount of residual water in the oil is determined using the Dean-Stark apparatus in accordance with the GOST 2477-2014 standards. The oil sample used in this article is heavy emulsified oil from the Umbaki field, and its physical-chemical properties are presented in the Table 1.

The empirical modeling of the demulsification process was carried out using the OriginLab 2024 software package.

Table 1. Physical-chemical properties of Umbaki oil
Tabela 1. Właściwości fizykochemiczne ropy naftowej Umbaki

Parameter	Value	Determination method
Density 20°C [kg/m^3]	962.5	ASTM D1298 (Hydrometer method)
Viscosity 20°C [mP·s]	2246	ASTM D445 (Capillary viscometer)
Water content [% *m*/*m*]	31	ASTM D4006 (Dean-Stark method)
Chloride salts content [mg/L]	152.1	ASTM D3230 (Conductometric method)
Mechanical impurities content [% *m*/*m*]	1.9	GOST 6370 or filtration method
Resins content [% *m*/*m*]	9.7	ASTM D2007 (Solvent extraction method)
Asphaltenes content [% *m*/*m*]	5.0	ASTM D6560 (*n*-heptane precipitation)
Paraffins content [% *m*/*m*]	6.2	UOP 46-64 or gravimetric method after solvent crystallization
Freezing temperature [°C]	16	ASTM D2386 (Cooling bath method)

Regression analysis, including polynomial and exponential fitting, was applied to determine mathematical relationships between key experimental variables such as temperature, demulsifier concentration, and residual water content. For enhanced visualization and analysis of experimental data, the Advanced Grapher tool (version 2.2, Alentum Software) was employed, particularly in plotting three-dimensional surface graphs. Additionally, Microsoft Excel was used for statistical evaluation, data tabulation, and generation of auxiliary graphs. The model coefficients were estimated using the least squares method, and the quality of fit was assessed by *R*-squared (R^2) values and standard error metrics.

Results and Discussion

Since the oil sample used for the research exhibits the characteristics of a stable emulsified oil, it is capable of retaining reservoir water for extended periods. The high content of asphaltenes, resins, and paraffin components, as well as the considerable amount of salts, enhances the stability of the emulsion. Therefore, the research initially focused on studying the effect of temperature alone on the stability of the emulsion. Preliminary experiments at 20 and 30°C demonstrated no significant influence on the stability of such emulsions, and the corresponding data are therefore not included; subsequent investigations were carried out at higher temperatures. The demulsification process of 31% water-saturated Umbaki oil was examined at 40, 50, 60, and 70°C, and the results are presented in Table 2.

It can be observed from Table 2 that the effect of temperature on the stability of the Umbaki water-oil emulsion is not particularly strong. Test experiments conducted over a 2-hour period indicated that, after demulsification at 70°C, the amount of residual water was 18.9%, and the ballast water amounted to 14.9%. The influence of temperature alone is insufficient to break down the stability of the emulsion formed by this type of heavy oil, as residual and ballast water content remain considerably high. Therefore, it becomes necessary to apply demulsifiers that reduce surface tension alongside temperature.

Subsequent investigations were carried out using ND-12 and Dissolvan-4411 demulsifiers at concentrations of 200, 400, and 600 g/t at 40°C. The results are presented in Figure 1, in which UB denotes Umbaki ballast water and UR denotes Umbaki residual water.

The results presented in Figure 1 indicate that the application of the reagents, in combination with elevated temperature, enhanced the rate of demulsification. At a concentration of 600 g/t of Dissolvan-4411 (Figure 1B), the minimum amount of ballast water achieved during demulsification was 14.07%,

Table 2. Demulsification of Umbaki oil at various temperatures
Tabela 2. Deemulgacja ropy naftowej Umbaki w różnych temperaturach

Temperature [°C]	Demulsification time [h]				Amount of ballast water [%]
	0.5	1.0	1.5	2.0	
	Amount of separated water [%]				
40	1.7	2.1	2.7	3.1	28.8
50	2.7	3.2	4.1	4.6	27.6
60	3.5	5.7	8.3	9.6	23.6
70	7.2	12.4	14.5	18.9	14.9

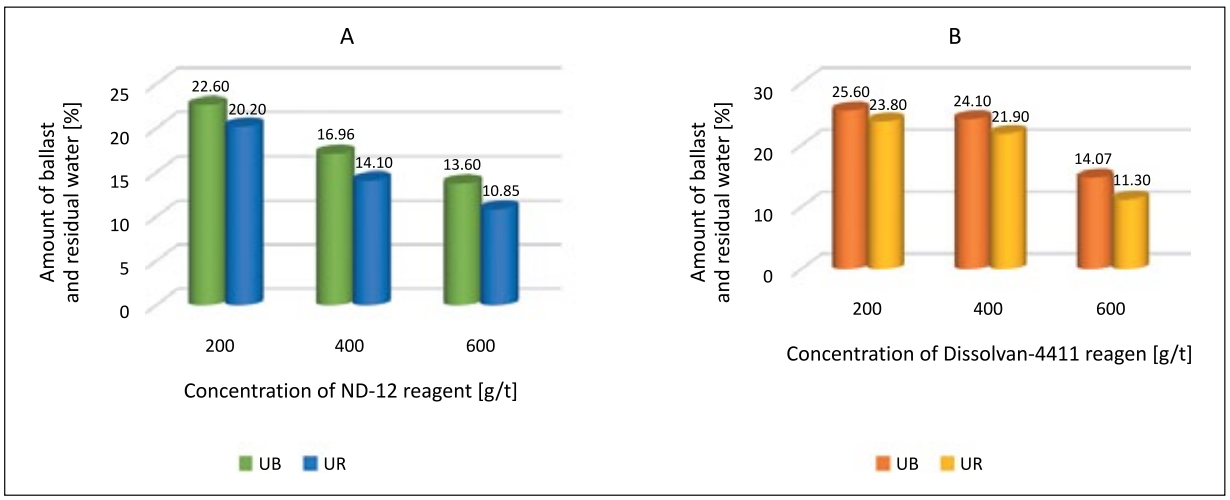

Figure 1. Dependence of the amount of ballast (UB) and residual water (UR) on the concentration of (A) ND-12 and (B) Dissolvan-4411 reagents during demulsification at 40°C

Rysunek 1. Zależność ilości wody balastowej (UB) i resztkowej (UR) od stężenia środków (A) ND-12 i (B) Dissolvan-4411 podczas demulgacji w temperaturze 40°C

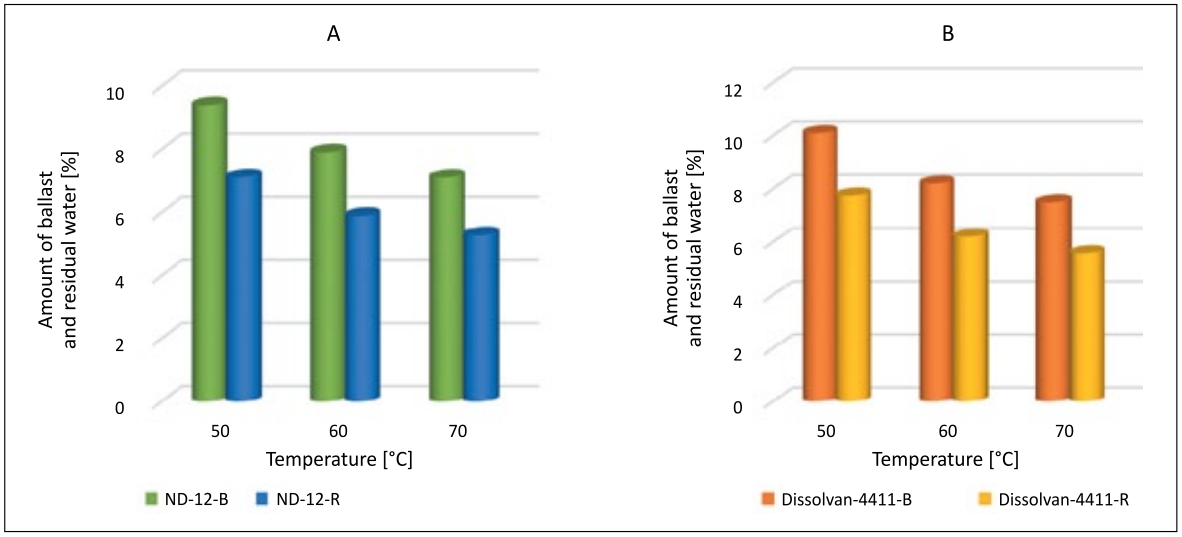

Figure 2. Dependence of residual water and ballast water on temperatures of 50, 60, and 70°C at a concentration of 600 g/t: (A) ND-12 reagent and (B) Dissolvan-4411 reagent

Rysunek 2. Zależność zawartości wody resztkowej i balastowej od temperatur 50, 60 i 70°C przy stężeniu 600 g/t: (A) reagent ND-12 oraz (B) reagent Dissolvan-4411

while the residual water content was 11.3%. In comparison, treatment with ND-12 at the same concentration (Figure 1A) resulted in 13.6% ballast water and 10.85% residual water. However, as the results obtained at 40°C did not fully satisfy the performance requirements, further investigations were carried out at 50, 60, and 70°C using a fixed concentration of 600 g/t for both Dissolvan-4411 and ND-12 demulsifiers. The corresponding data are presented in Figure 2.

As shown in Figure 2, the efficiency of demulsification increased with rising temperature in the range of 50–70°C. The increase in temperature also raises the activation energy, thereby enhancing the action of the demulsifier. Consequently, the results obtained during the demulsification process at elevated temperatures in the presence of a demulsifier were more effective. At the optimal concentration of Dissolvan-4411, at 50°C the amount of ballast water was 10.1% and the residual water was 7.5%; at 60°C the ballast water was 8.2% and the residual water was 6.2%; and at 70°C the ballast water was 7.5% and the residual water was 5.58%. Evidently, the efficiency of Dissolvan-4411 was enhanced at 70°C. At 600 g/t concentration of ND-12, at 50 °C the ballast water was 9.4% and the residual water was 7.11%; at 60°C the ballast water was 7.9% and the residual water was 5.89%; and at 70°C the ballast water was 7.1% and the residual water was 5.27%. Based on these results, it can be concluded that at 70°C the ND-12 demulsifier exhibited higher effectiveness compared

with Dissolvan-4411. However, the results obtained for both demulsifiers at 70°C still did not meet the requirements for oil preparation under field conditions. Therefore, two Series A compositions were prepared on the basis of both demulsifiers, and their formulations are presented in Table 3.

Table 3. Composition and ratios of compositions (by volume)
Tabela 3. Skład i proporcje składników (objętościowo)

A-1	ND-12 + Gossypol resin + isopropanol	4 : 1.5 : 0.5
A-2	Dissolvan-4411 + Gossypol resin + isopropanol	4 : 1.5 : 0.5

The A-1 series composition consists of the ND-12 demulsifier, Gossypol resin as an anticorrosion agent, and isopropanol as a surfactant (Jiang et al., 2018). Isopropanol facilitates the dissolution and disruption of the structures surrounding the dispersive phases, while the anticorrosion agent has been demonstrated – through both theoretical analyses and experimental studies – to exhibit the most effective performance when applied in combination with the demulsifier (Roodbari et al., 2011; Xia et al., 2023). The A-2 series composition comprises Dissolvan-4411, Gossypol resin, and isopropanol as a surfactant.

Experimental investigations on the demulsification of Umbaki crude oil using the A-1 and A-2 compositions at concentrations of 200, 400, and 600 g/t at 40°C were performed, and the results are presented in Table 4.

Table 4. Comparative results of oil demulsification with the A-1 and A-2 compositions at 40°C
Tabela 4. Wyniki porównawcze deemulgacji ropy naftowej przy użyciu kompozycji A-1 i A-2 w temperaturze 40°C

Composition	Water content [%]	Concentration [g/t]	Residual water content [%]	Ballast water [%]
A-1	31	200	19.3	21.9
		400	13.4	16.3
		600	6.8	8.9
A-2		200	20.5	22.9
		400	15.2	18.1
		600	8.6	11.1

Based on the results presented in Table 4, it can be observed that the most effective concentrations of the compositions coincide with those of the individual reagents, thereby enabling a valid comparative analysis. In comparison with the results obtained for the individual reagents at 40°C, the compositions demonstrated superior efficiency in the demulsification process, with the A-1 composition exhibiting greater effectiveness than A-2. To extend the comparative analysis, additional experiments were carried out on emulsions with an initial water content of 31%, evaluating the performance of the A-1 and A-2 compositions at concentrations of 300, 400, 500, and 600 g/t at temperatures of 50, 60, and 70°C. The outcomes of these experiments are presented in Tables 5 and 6.

Table 5 shows that under the influence of the A-1 composition, at a temperature of 50°C and a concentration of 600 g/t, the ballast water content was 5.3%, while the residual water content was 12.5%. At 60°C and the same concentration, the ballast

Table 5. Demulsification of Umbaki oil sample with A-1 composition
Tabela 5. Demulgowanie próbki ropy Umbaki za pomocą kompozycji A-1

Deemulsification temperature [°C]	Concentration [g/t]	Residual water content [%]	Ballast water [%]
50	300	27.40	10.96
	400	18.50	7.67
	500	15.80	6.63
	600	10.06	4.33
60	300	18.60	7.71
	400	16.40	6.86
	500	10.50	4.50
	600	5.14	2.26
70	300	2.50	1.11
	400	1.60	0.71
	500	0.50	0.22
	600	0.28	0.13

Table 6. Demulsification of Umbaki oil sample with A-2 composition
Tabela 6. Demulgowanie próbki ropy Umbaki za pomocą kompozycji A-2

Deemulsification temperature [°C]	Concentration [g/t]	Residual water content [%]	Ballast water [%]
50	300	29.20	11.6
	400	21.40	8.8
	500	17.90	7.4
	600	12.48	5.3
60	300	21.90	8.9
	400	19.40	8.0
	500	13.60	5.8
	600	7.54	3.3
70	300	4.70	2.1
	400	3.80	1.7
	500	2.00	0.9
	600	0.79	0.4

water was 3.3% and the residual water 7.5%. At 70°C, under identical conditions, the ballast water decreased to 0.4%, while the residual water content was 0.8%. According to Table 6, under the influence of the A-2 composition, at a temperature of 50°C and a concentration of 600 g/t, the ballast water content was 5.3% and the residual water content 12.5%. At 60°C, the ballast water amounted to 3.3% and the residual water to 7.5%. At 70°C, the ballast water was reduced to 0.4%, while the residual water reached 0.8%. The results obtained for both compositions at 70°C meet the requirements for residual water content in oil preparation for transportation under field conditions. However, the A-1 composition consistently exhibited superior effectiveness compared with the A-2 composition across all tested temperatures. Therefore, the use of the A-1 composition under field conditions is expected to provide more effective results while reducing both reagent consumption and energy costs. Thus, the demulsification of difficult to break emulsions, such as those from the Umbaki field, is most effectively achieved at 70°C.

Since the A-1 composition demonstrated the highest effectiveness, three-dimensional surface plots were constructed to illustrate the dependence of residual and ballast water content in Umbaki oil on demulsification time, temperature, and reagent concentration. These dependencies are depicted in Figures 3–6. In these plots, the X-axis represents the demulsification time [min], the Y-axis indicates the residual or ballast water content [%], and the Z-axis shows the reagent concentration [g/t]. The color legend reflects the distribution ranges of the experimentally measured values, thereby providing enhanced visual interpretation.

From the 3D graphs, it can be observed that the surface areas corresponding to ballast and residual water content are represented in different colors. The 0–5% interval indicates the lowest water content; therefore, the color region occupying the largest surface area within this range reflects the most favorable combination of composition dosage, time, and temperature. This decreasing trend in both ballast water and residual water content is particularly evident at 70°C, as shown in Figures 3 and 6.

In recent years, empirical modeling has increasingly employed non-linear numerical series and differential equations, including multi-dimensional forms. The preference for empirical over theoretical modeling arises from the fact that many problems lack robust theoretical foundations or are constrained by existing theories, which are often insufficient to provide satisfactory solutions. Moreover, theoretically derived models are typically more computationally demanding, whereas empirically derived models can offer faster and more practical solutions. The development of empirical or semi-empirical

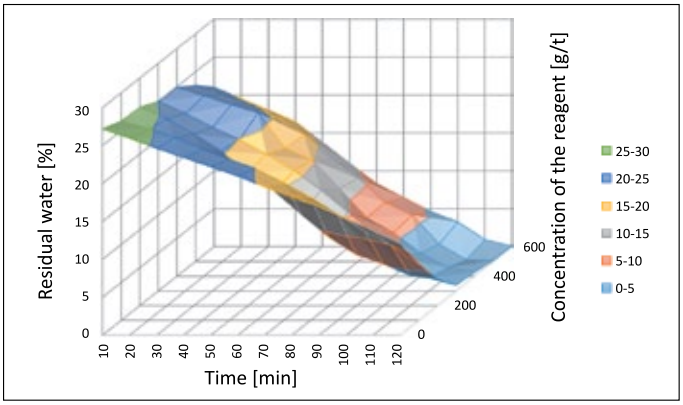

Figure 4. Three-dimensional surface plot of residual water content as a function of demulsification time and reagent concentration for the A-1 composition at 70°C in Umbaki oil

Rysunek 4. Trójwymiarowy wykres powierzchniowy zawartości wody resztkowej w funkcji czasu deemulgacji i kompozycji A-1 w temperaturze 70°C w ropie naftowej Umbaki

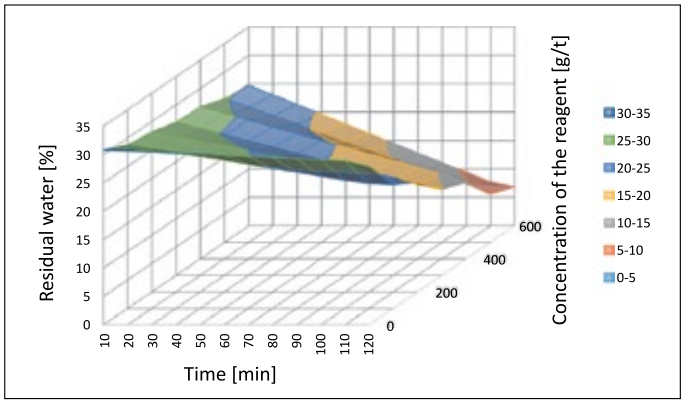

Figure 3. Three-dimensional surface plot of residual water content as a function of demulsification time and concentration of the A-1 composition at 40°C in Umbaki oil

Rysunek 3. Trójwymiarowy wykres powierzchniowy zawartości wody resztkowej w funkcji czasu deemulgacji i stężenia kompozycji A-1 w temperaturze 40°C w ropie naftowej Umbaki

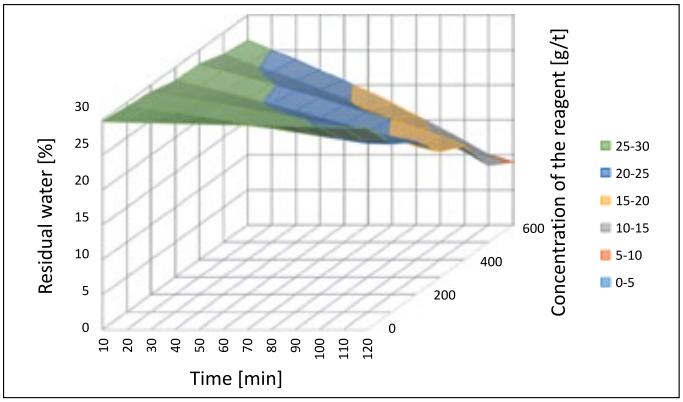

Figure 5. Three-dimensional surface plot of ballast water content as a function of demulsification time and reagent concentration for the A-1 composition at 40°C in Umbaki oil

Rysunek 5. Trójwymiarowy wykres powierzchniowy zawartości wody balastowej w funkcji czasu deemulgacji i stężenia kompozycji A-1 w temperaturze 40°C w ropie naftowej Umbaki

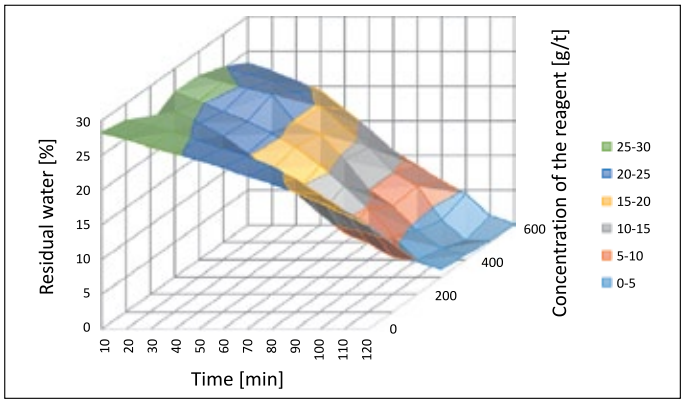

Figure 6. Three-dimensional surface plot of ballast water content as a function of demulsification time and reagent concentration for the A-1 composition at 70°C in Umbaki oil

Rysunek 6. Trójwymiarowy wykres powierzchniowy zawartości wody balastowej w funkcji czasu deemulgacji i stężenia kompozycji A-1 w temperaturze 70°C w ropie naftowej Umbaki

models for complex physical phenomena requires a comprehensive analysis of experimental curves due to their inherent complexity. This necessity stems from the fact that constructing a phenomenological model for such processes, which are characterized by continuous changes in flow behavior, is either theoretically unresolved or highly intricate. For many complex phenomena, it is essential to formulate empirical models across a broad range of parameter variability with minimal computational cost. In such cases, piecewise approximations in the form of empirical equations are often applied to specific flow regions. The main challenge in constructing empirical models for complex physical phenomena lies in the detailed analysis of experimental curves over the entire range and in the adjustments required to identify characteristic points and transitional behaviors.

It is known that the following conditions must be fulfilled in order to establish the empirical model $Y(x) = F(x)$ that describes the experimental research:

- Ensuring the boundary conditions of the problem for the experimental curve;

$$Y(x)\big|_{x=0} = Y_0(x) \ldots Y(x)\big|_{x\to\infty} = Y_\infty(x) \tag{3}$$

- Specifying characteristic points on the experimental curve (such as inflection points, extremum points, regions of increase or decrease of the curve, etc.);
- Ensuring steady-state conditions in certain regions of the curve.

The construction of the final model and the selection of smoothing functions for different regions of the curve involve choosing smoothing functions that match the form of the experimental curve, adhering to all boundary conditions, and successfully estimating the coefficients of the unknowns included in the equation.

The factors influencing the separation of water from the oil dispersion system are the duration of the demulsification process, the reagent dosage, and the temperature. In Umbaki oil, temperature is considered the most significant factor. The polynomial regression model representing the influence of all three factors is expressed as follows:

$$y = A_0 + A_1 \cdot x_1 + A_2 \cdot x_2 + A_3 \cdot x_3 \tag{4}$$

where:

x_1 – denotes temperature [°C],
x_2 – denotes reagent dosage [g/t],
x_3 – denotes time [h],
A_0 – intercept (constant term),
A_1, A_2, A_3 – regression coefficients representing the influence of each corresponding factor on the response variable (y).

The coefficients and standard errors obtained from the polynomial regression model applied to the demulsification data of Umbaki oil are presented in Table 7.

As shown in Table 7, the x_1, x_2, and x_3 variables (corresponding to time, reagent dosage, and temperature) demonstrate statistically significant coefficients in the polynomial model. The statistical performance of the emulsification model for Umbaki oil using the A-1 composition is summarized in Table 8. According to Table 8, the model exhibits a high correlation coefficient ($R = 0.939$) and an acceptable standard error, confirming the adequacy of the polynomial approximation.

The curve of experimental indicators and the curve of calculated points based on the polynomial model are presented in Figure 7.

Table 7. Indicators of the polynomial model in Umbaki oil

Tabela 7. Wskaźniki modelu wielomianowego w ropie Umbaki

	Coefficients	Standard error
y-intercept	45.662	0.438
x_1 variable (t)	–0.127	0.003
x_2 variable (G)	–0.019	0.001
x_3 variable (T)	–0.253	0.007
t – demulsification time (h), G – reagent dosage (g/t), T – temperature (°C)		

Table 8. Statistical indicators of the emulsification process model of Umbaki oil with A-1

Tabela 8. Wskaźniki statystyczne modelu procesu deemulgacji ropy naftowej Umbaki z użyciem kompozycji A-1

Regression statistics	
Multiple R	0.939
R-squared	0.883
Adjusted R-squared	0.881
Standard error	2.657
Number of experiments	504

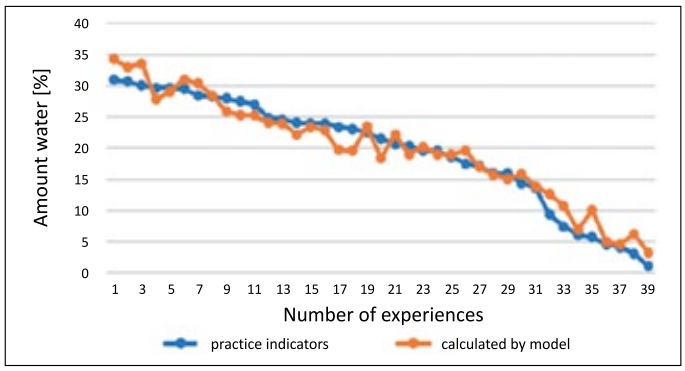

Figure 7. Separation of Umbaki water-oil emulsion
Rysunek 7. Rozdział emulsji wodno-olejowej Umbaki

Figure 7 illustrates the comparison between the experimental results obtained from bottle-test measurements and the values calculated using the polynomial model. The close agreement of these two curves confirms the model's accuracy and highlights its potential to reliably characterize the demulsification behavior of resinous crude oil emulsions under varying conditions. Although the reliability of the polynomial model is sufficiently high and it adequately reflects the dynamics of residual water variation, an additional empirical model based on exponential equations will also be developed. Figure 8 presents the dynamics of residual water content as a function of oil separation duration at 20°C. Similar graphs have been constructed for other temperatures (30, 40, 50, 60, and 70°C) at different concentrations of the A-1 composition (0, 100, 300, and 600 g/t).

This dependency:

$$y = C_0 \cdot \exp(b \cdot t) \quad (5)$$

is presented in the form of a model. The lowest reliability coefficient for this dependency is 0.91, while the others exceed 0.97, confirming the reliability of the selected formula.

The coefficient C_0 (in model 5 at the first level) represents the initial amount of water present in the oil emulsion. The variations in the initial amount of water found in Figure 4 are subject to systematic errors (due to factors such as the accuracy of experiments, measurements, calculations, etc.). Therefore, the average value of the initial water content has been calculated and is presented in Figure 9 illustrating this dependency for each temperature.

Subsequently, the coefficient b was recalculated using the mentioned average values. Given the strong dependence of the coefficient a on temperature, it should be expressed by a separate equation and include the parameter T in model (6).

$$y = y_0 + A \cdot \exp(-(T/t_1)^b)) \quad (6)$$

A more accurate model equation was selected. Here, y_0, t_1, and b are the coefficients of this dependency model. The values of the obtained coefficients are recorded in equation (7).

$$C_0 = 28.5128 + 3.007 \cdot \exp(-T/41.20018)^{5.19265})$$
$$b = b_0 + B_1 \cdot G \quad (7)$$

To obtain a more precise value for the coefficient b in model (6) and to incorporate the parameter for the composition amount into model (6), a simple linear equation (a polynomial with one term and a free coefficient) was employed (Figure 10). As the coefficients of equation (7) (b_0, B_1) vary with temperature, approximation curves of their dependence on temperature were analyzed, and equations expressing this relationship were determined.

Here, G represents the concentration of the composition. The dependencies of the intercept and coefficient B in equation (7) on temperature are illustrated in Figures 11 and 12, respectively, and have been approximated using a second-order polynomial (8).

$$y = \text{Intercept} + B_1 \cdot T + B_2 \cdot T^2 \quad (8)$$

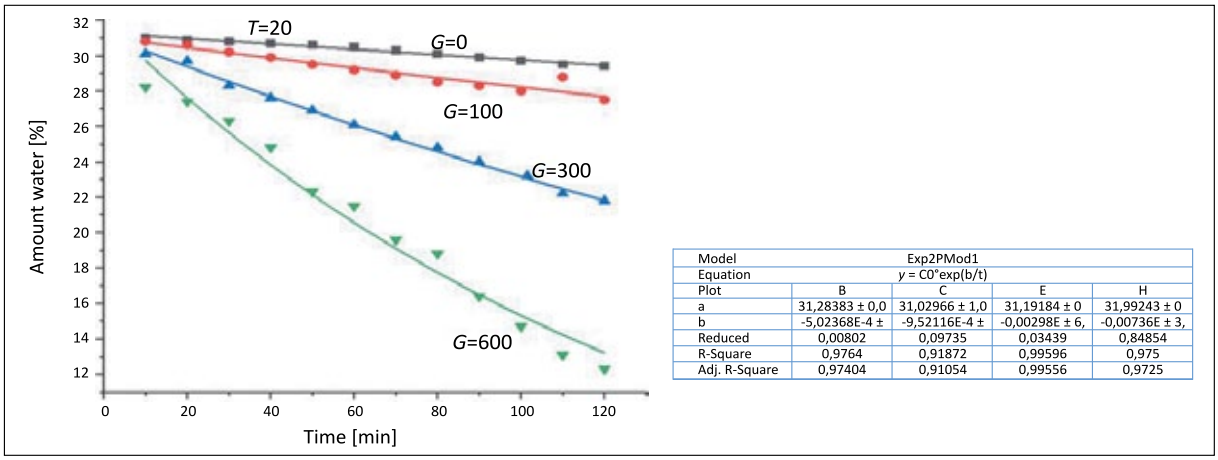

Model	Exp2PMod1			
Equation	y = C0*exp(b/t)			
Plot	B	C	E	H
a	31,28383 ± 0,0	31,02966 ± 1,0	31,19184 ± 0	31,99243 ± 0
b	-5,02368E-4 ±	-9,52116E-4 ±	-0,00298E ± 6,	-0,00736E ± 3,
Reduced	0,00802	0,09735	0,03439	0,84854
R-Square	0,9764	0,91872	0,99596	0,975
Adj. R-Square	0,97404	0,91054	0,99556	0,9725

Figure 8. Dependence of residual water separation on process duration at T = 20°C for different concentrations of the A-1 composition (G = 0, 100, 300, and 600 g/t)
Rysunek 8. Zależność wydzielania wody resztkowej od czasu trwania procesu w temperaturze T = 20°C dla różnych stężeń kompozycji A-1 (G = 0, 100, 300 i 600 g/t)

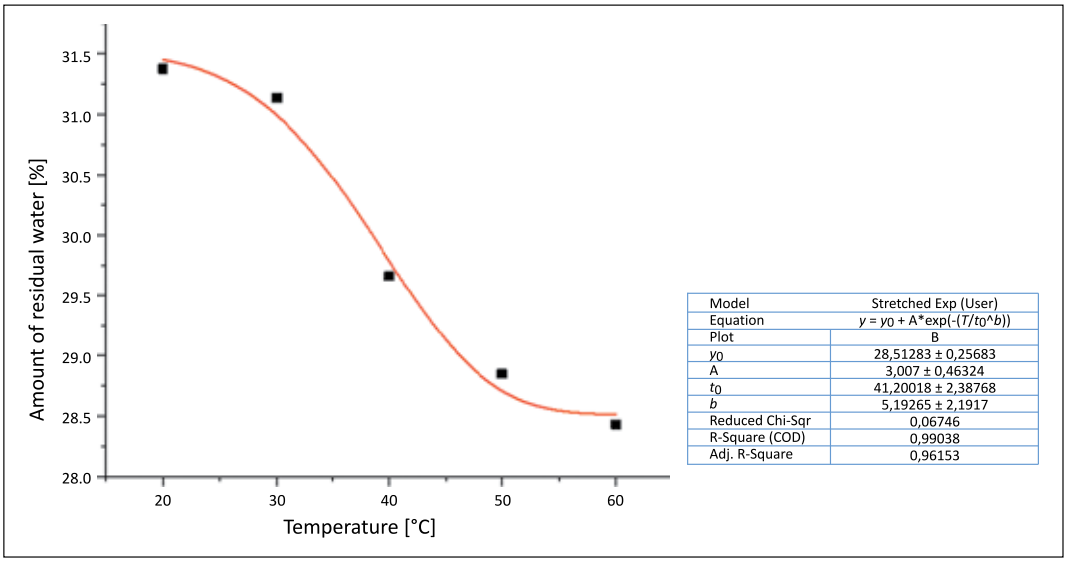

Model	Stretched Exp (User)
Equation	$y = y_0 + A*\exp(-(T/t_0\text{^}b))$
Plot	B
y_0	28,51283 ± 0,25683
A	3,007 ± 0,46324
t_0	41,20018 ± 2,38768
b	5,19265 ± 2,1917
Reduced Chi-Sqr	0,06746
R-Square (COD)	0,99038
Adj. R-Square	0,96153

Figure 9. Dependency of the initial amount of residual water on temperature
Rysunek 9. Zależność początkowej ilości wody resztkowej od temperatury

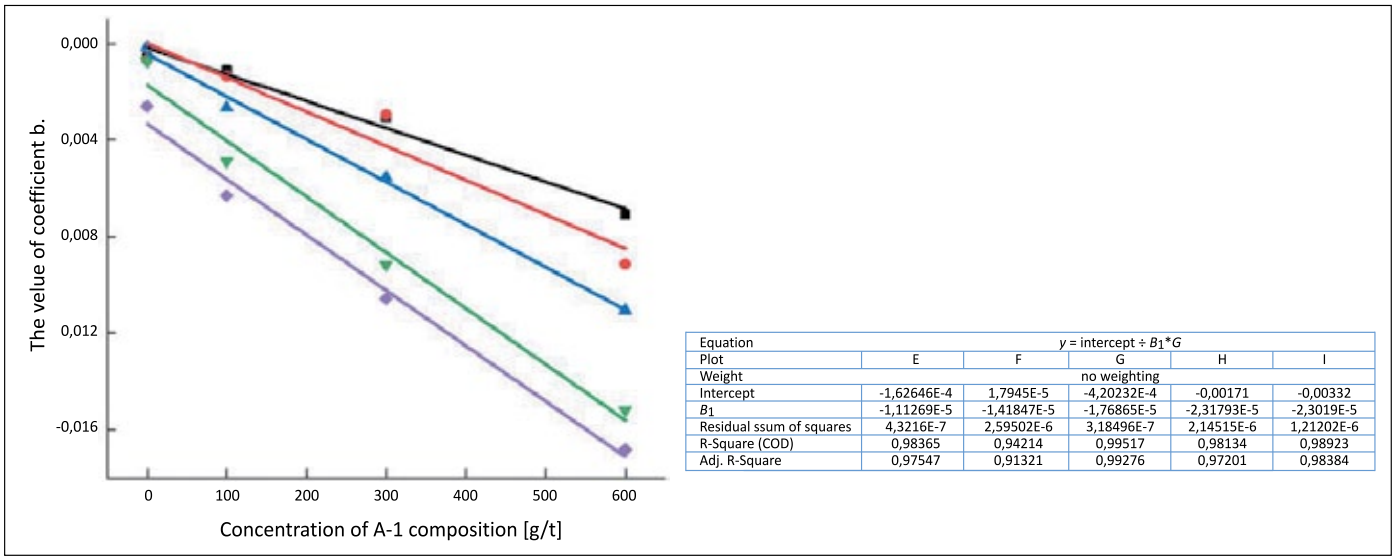

Equation	y = intercept ÷ B_1*G				
Plot	E	F	G	H	I
Weight	no weighting				
Intercept	-1,62646E-4	1,7945E-5	-4,20232E-4	-0,00171	-0,00332
B_1	-1,11269E-5	-1,41847E-5	-1,76865E-5	-2,31793E-5	-2,3019E-5
Residual ssum of squares	4,3216E-7	2,59502E-6	3,18496E-7	2,14515E-6	1,21202E-6
R-Square (COD)	0,98365	0,94214	0,99517	0,98134	0,98923
Adj. R-Square	0,97547	0,91321	0,99276	0,97201	0,98384

Figure 10. Determining the dependence of the coefficient b in model (6) on the amount of composition
Rysunek 10. Określenie zależności współczynnika b w modelu (6) od ilości kompozycji

Thus, the final model of the separation process for Umbaki oil, taking into account the coefficients obtained at each stage and the structure of these equations, is as follows:

$$y = C_0 \cdot \exp(b \cdot t)$$

a-T dependency, is defined as $a = y_0 + A \cdot \exp(-(T/t_1)^b)$

$$y = 28.5128 + 3.007 \cdot \exp(-T/41.20018)^{5.19265})$$

$$b = b_0 + B_1 \cdot G$$

$$b_0 = (-0.00234 + 1.7313e\text{-}4 \cdot t\text{-}3.16909E\text{-}6 \cdot T^2)$$

$$B_1 = (-2.82614e\text{-}7 - 5.81793e\text{-}9 \cdot T + 3.17503e\text{-}9 \cdot T^2)$$

$$b = (-0.00234 + 1.7313e\text{-}4 \cdot t\text{-}3.16909E\text{-}6 \cdot T^2) + \\ + (-2.82614e\text{-}7 - 5.81793e\text{-}9 \cdot T + 3.17503e\text{-}9 \cdot T^2) \cdot G$$

$$y = 28.5128 + 3.007 \cdot \exp(-T/41.20018)^{5.19265}) \cdot \\ \cdot \exp((-0.00234 + 1.7313e\text{-}4 \cdot t\text{-}3.16909E\text{-}6 \cdot T^2) + \\ + (-2.82614e\text{-}7 - 5.81793e\text{-}9 \cdot T + \\ + 3.17503e\text{-}9 \cdot T^2) \cdot G)) \cdot t \qquad (9)$$

The proposed empirical model (9) fully characterizes the demulsification process of Umbaki oil at any temperature, within the concentration range of the A-1 composition (0–600 g/t), and for process durations ranging from 0 to 120 minutes. It includes all necessary parameters for predictive modelling. The calculations replicate the profile of the experimental curve, and the reliability of the applied approximation equations is not lower than $R^2 = 0.91$, $R^2 = 0.91$, $R^2 = 0.91$, with most cases having $R^2 = 0.99$, $R^2 = 0.99$, $R^2 = 0.99$. The relative error is 12%.

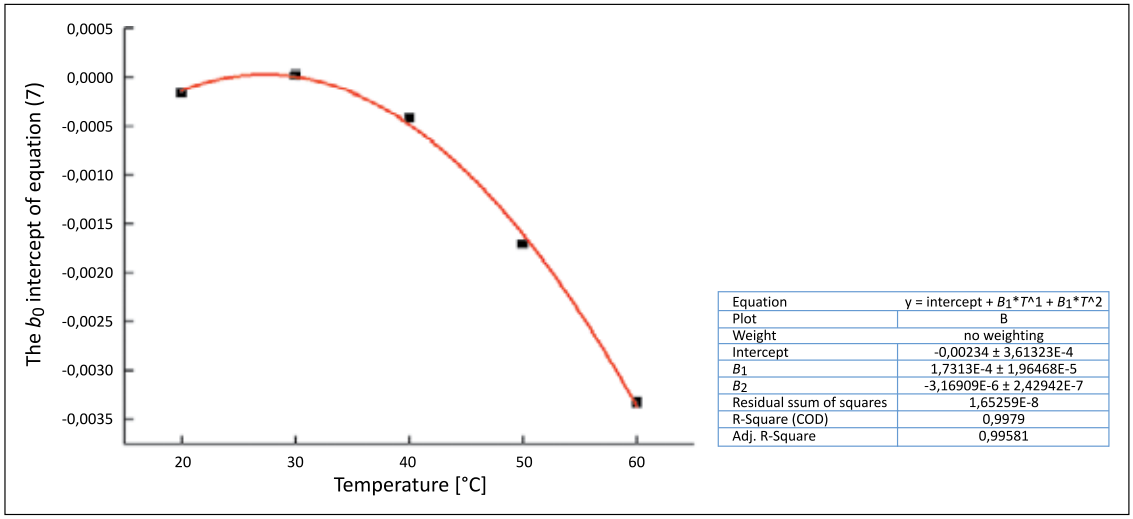

Equation	y = intercept + B_1*T^1 + B_1*T^2
Plot	B
Weight	no weighting
Intercept	-0,00234 ± 3,61323E-4
B_1	1,7313E-4 ± 1,96468E-5
B_2	-3,16909E-6 ± 2,42942E-7
Residual ssum of squares	1,65259E-8
R-Square (COD)	0,9979
Adj. R-Square	0,99581

Figure 11. Temperature dependence of the intercept in equation (7) (b_0)
Rysunek 11. Zależność wyrazu wolnego w równaniu (7) (b_0) od temperatury

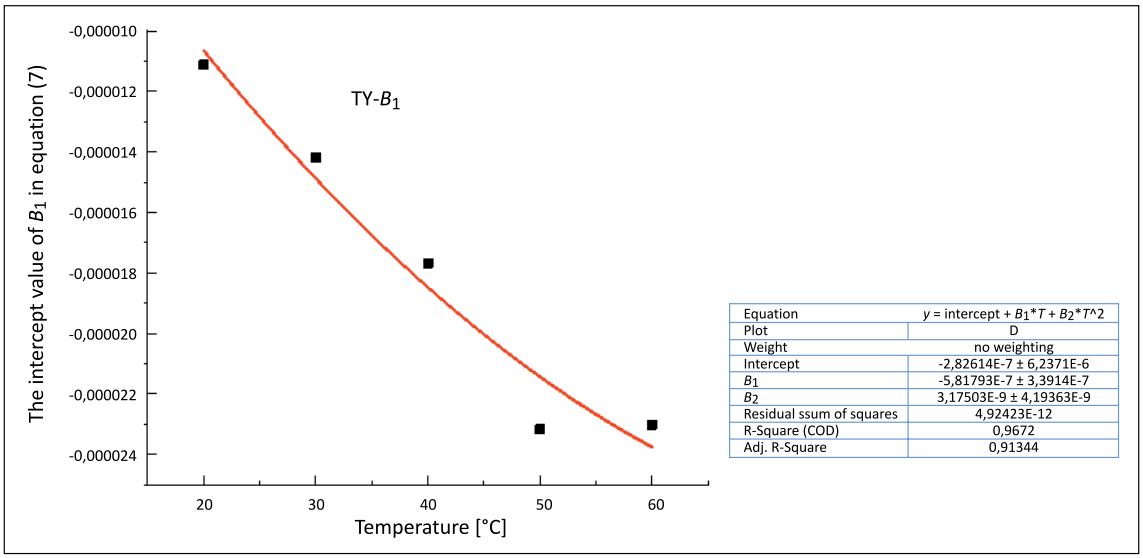

Equation	y = intercept + B_1*T + B_2*T^2
Plot	D
Weight	no weighting
Intercept	-2,82614E-7 ± 6,2371E-6
B_1	-5,81793E-7 ± 3,3914E-7
B_2	3,17503E-9 ± 4,19363E-9
Residual ssum of squares	4,92423E-12
R-Square (COD)	0,9672
Adj. R-Square	0,91344

Figure 12. Temperature dependence of the intercept in equation (7) (B_1)
Rysunek 12. Zależność współczynnika przecięcia w równaniu (7) (B_1) od temperatury

Benchmarking A-1 and A-2 compositions against established demulsification agents

The efficiency of demulsifier formulations in breaking stable water-in-oil emulsions, particularly in heavy crude systems, depends on multiple physicochemical parameters, including temperature, dosage, molecular structure, and compatibility with the specific crude oil matrix. In our study, we systematically evaluated two composite formulations – A-1 and A-2 – across a range of temperatures (50°C to 70°C) and concentrations (300 to 600 g/t), using the bottle test method in accordance with industry standards. These experimental results were compared with published data by Roodbari et al. (2011), who investigated the demulsification behavior of a series of nonionic surfactants (Tweens 20, 40, 60, 80, and 85) in heavy crude oil emulsions. Such a comparison provides critical context for assessing the relative performance and potential field applicability of the A-1 and A-2 compositions. According to our experimental results, both formulations exhibited concentration- and temperature-dependent demulsification performance, with A-1 demonstrating superior water separation under nearly all tested conditions. At 70°C and 600 g/t dosage, the A-1 composition achieved a residual water content of just 0.28%, while A-2 reached 0.79%. This indicates highly efficient phase separation and minimal retention of emulsified water. Additionally, the ballast water content – a secondary indicator of phase purity – was reduced to 0.13% for A-1 and 0.4% for A-2, reinforcing the high degree of demulsifier effectiveness and the advanced breakdown of the interfacial film surrounding water droplets.

In comparison, Roodbari et al. (2011) tested Tween-based nonionic surfactants within a concentration range of 300–900 ppm, with their optimal results typically observed at 400–600 ppm, depending on the Tween type. Their study, which involved emulsions formed with heavy crude oil from the Azadegan field in Iran, demonstrated reasonable water separation efficiency. For instance, Tween 20 showed good demulsification at 400 ppm, and Tween 85 at 600 ppm. However, in most cases, the residual water content remained above 2%, with no indication of achieving sub-1% values. Although the exact initial water content and emulsion stability parameters differ between the two studies, it is clear that the A-series formulations, particularly A-1, produced a markedly lower residual water percentage under comparable thermal and dosage conditions. This difference may be attributed to several factors. First, the compositional complexity of A-1 and A-2 involves synergistic chemical interactions between their components – likely including paraffin inhibitors, surfactants with tailored hydrophilic-lipophilic balance (HLB), and potentially co-solvents that modify interfacial tension and coalescence rates. Unlike single-component Tweens, which rely primarily on polyoxyethylene chains and ester linkages for their demulsification activity, the A-series formulations appear to exhibit multifunctional behavior, enhancing both the penetration into the oil-water interface and the rupture of interfacial films. In addition, the tailoring of A-1 formulation toward the specific properties of Umbaki crude oil – which is known for its high paraffin and resin content – may have contributed to the observed improvement in separation efficiency.

Another critical distinction lies in the ballast water parameter, which is often overlooked in many demulsification studies. Ballast water refers to a phase that may remain after incomplete separation – a mixture of water with suspended oil or emulsion fragments. In our work, the inclusion of this metric allows for a more nuanced understanding of separation completeness. Roodbari et al. (2011) do not report ballast water values, but the clarity and sharpness of phase boundaries described in their results suggest that minor entrainment may still exist, particularly in mid-range dosages. It is also important to recognize that while Roodbari et al. (2011) emphasize the role of HLB number and polyoxyethylene content in demulsifier efficiency, our findings suggest that molecular synergy and oil-specific customization can be equally, if not more, impactful. For instance, despite A-2 being less effective than A-1, it still consistently outperformed the Tweens across most comparable conditions, especially at temperatures above 60°C. This implies that even partially optimized composite formulations can surpass traditional single-component surfactants when engineered appropriately for the target crude system. A further point of comparison relates to the temperature dependency of demulsification. Both studies confirm that increasing temperature enhances demulsifier activity, as elevated thermal energy reduces interfacial viscosity and promotes droplet coalescence (Wang et al., 2017; Zhao et al., 2021). However, while Tween surfactants require higher ppm dosages to achieve moderate reductions in residual water at 70°C, our A-1 composition achieved outstanding results (0.28% residual water) at only 600 g/t, which is within practical dosage limits for industrial application. This not only highlights efficiency but also suggests potential economic advantages due to reduced chemical consumption.

Importantly, our study is not intended to discount the contributions of Roodbari et al. (2011) who provided a valuable benchmark for the use of Tweens in heavy oil demulsification. Their work helped define the relationship between surfactant structure and performance, particularly the importance of hydrophilic-lipophilic balance (HLB) and chain length. Rather, our findings build upon this foundation and demonstrate how multicomponent systems like A-1 can be developed to achieve improved performance in specific crude oil environments. In conclusion, both A-1 and A-2 compositions demonstrate high demulsification potential, with A-1 achieving industry-relevant performance levels under relatively mild laboratory conditions. Compared to the benchmark Tween-based demulsifiers reported by Roodbari et al. (2011) our compositions provided lower residual water contents, better phase clarity, and reduced ballast water, all of which indicate more complete and efficient separation. These results support the viability of the A-series formulations for use in heavy oil processing and warrant further evaluation under field conditions to validate their operational robustness (Roodbari et al., 2011).

As a second comparative reference, demulsifiers synthesized from recycled polyethylene terephthalate (PET), namely as reported by Abdullah et al. (2021), were considered. These reagents, based on esterified nonionic surfactants, demonstrated promising demulsification performance in heavy crude oil emulsions. Optimal results were achieved at 45–65°C and concentrations ranging from 200 to 1000 ppm, with the lowest reported residual water content reaching approximately 0.6–0.9%. In the present study, the performance of two newly developed compositions – A-1 (ND-12 + gossypol resin + isopropanol) and A-2 (Dissolvan-4411 + gossypol resin + isopropanol), both in a 4:1.5:0.5 ratio – was assessed under varying temperature and dosage conditions. The results showed that both compositions effectively reduced the residual water content in the treated oil, especially at elevated temperatures and optimal dosages. Notably, the A-1 composition achieved a residual water content of just 0.28% at 70°C and 600 g/t, outperforming both the A-2 composition (0.79%) and the DOAT/DOAP (dioleic acid triethanolamine/dioleic acid pentaerythritol) series under comparable conditions.

While DOAT and DOAP offer a notable environmental advantage due to their derivation from recycled PET and exhibit favorable demulsification efficiency, their synthesis involves relatively complex polymer modification steps and esterification processes. In contrast, the A-series compositions proposed in this study are formulated from readily available industrial surfactants and gossypol resin, offering both operational simplicity and excellent demulsification performance. Thus, the outcome of this second comparative analysis indicates that although DOAT/DOAP-based demulsifiers are environmentally innovative, the A-1 formulation demonstrates superior efficiency in water separation, coupled with a simpler preparation pathway and high applicability in field operations. These findings support the potential of A-series demulsifiers as effective and scalable solutions for breaking stable water-in-oil emulsions in heavy crude oil treatment (Abdullah et al., 2021).

Conclusions

1. For the first time, the demulsification process of heavy oil, characterized by an aggregate-kinetically stable water-oil emulsion from SOCAR's Umbaki field, was studied. The effects of individual reagents, such as ND-12 and Dissolvan-4411 demulsifiers, at temperatures of 40, 50, 60, and 70°C, as well as new compositions A-1 and A-2, derived from these demulsifiers, were examined. Their optimal concentrations were determined. It was found that the optimal concentration for ND-12, Dissolvan-4411, A-1, and A-2 reagents at the highest temperature is 600 g/t.
2. The results of multiple experiments showed that at 70°C, after two hours of treatment, the residual and ballast water content in Umbaki oil, when treated with the optimal concentrations of ND-12 and Dissolvan-4411, was 5.27% and 7.1%, respectively, for ND-12, and 5.58% and 7.5% for Dissolvan-4411. However, at the same temperature, the residual and ballast water contents in the treated oil samples with the optimal concentrations of A-1 and A-2 compositions was significantly lower: 0.07% and 0.13% for residual water, and 0.3% and 0.4% for ballast water.
3. For the first time, a 3D graph was constructed to show the dependence of residual and ballast water amounts on demulsification time, temperature, and composition concentration for the A-1 composition, which demonstrated the highest effectiveness in demulsifying stable water-oil emulsions. The mathematical modeling of the results was carried out, and the use of this composition as an economically and environmentally efficient reagent in field conditions was proposed.
4. It should be noted that the developed empirical models are specific to the tested resinous Umbaki crude oil and should be interpreted as case-specific tools rather than universal predictive models. However, they provide valuable insights and comparative data for similar heavy oil emulsion systems.

References

Abdullah M.M.S., Al-Lohedan H.A., Atta A.M. 2021. Fabrication of new demulsifiers employing the waste polyethylene terephthalate and their demulsification efficiency for heavy crude oil emulsions. *Molecules*, 26(3): 589. DOI: 10.3390/molecules26030589.

Adams J.J. 2014. Asphaltene adsorption: a literature review. *Energy and Fuels*, 28: 2831–2856. DOI: 10.1021/ef500282p.

Ali M.F., Alqam M.H. 2000. The role of asphaltenes, resins and other solids in the stabilization of water in oil emulsions and its effects on oil production in Saudi oil fields. *Fuel*, 79(11): 1309–1316. DOI: 10.1016/S0016-2361(99)00268-9.

Bakhtizin R.N., Karimov R.M., Mastobaev B.N., 2016. The impact of high molecular weight components on rheological properties depending on the structural group and fractional composition of oil. *SOCAR Proceedings*, 1: 42–50.

Bourrel M., Passade-Boupat N. 2018. Crude Oil Surface Active Species: Consequences for Enhanced Oil Recovery and Emulsion Stability. *Energy & Fuels*, 32(3): 2642–2652. DOI: 10.1021/acs.energyfuels.7b03435.

Girard H.-L., Bourrianne P., Chen D., Jaishankar A., Vreeland J.L., Cohen R.E., McKinley G.H., 2020. Asphaltenes adsorption on functionalized solids. *Langmuir*, 36: 3894–3902. DOI: 10.1021/acs.langmuir.0c00029.

Gurbanov A.N., Sardarova I.Z., 2022. Optimization Problem of Measurements In Experimental Research of Gas-Lift Wells. *Applied and Computational Mathematics*, 2: 223–228.

Gurbanov A.N., Sardarova I.Z., Damirova J.R., 2021. Analysis of qas preperation processes for improvment of gas transportation technology. EUREKA: *Physics and Engineering*, 6: 48–56. DOI: 10.21303/2461-2021.002081.

Gurbanov G.R., Nurullayev V. K., Gasimzade A.V. 2024. The effect of formation temperature and constituent components on rheological parameters of water-oil emulsions. *Nafta-Gaz*, 80(5): 301–311. DOI: 10.18668/NG.2024.05.06.

Gurbanov H.R., Gasimzade A.V., 2022. Research of the impact of new compositions on the decomposition of stable water-oil emulsions of heavy oils. *Voprosy Khimii i Khimicheskoi Tekhnologii*, 6: 19–28. DOI: 10.32434/0321-4095-2022-145-6-19-28.

Iskandarov E.Kh., Baghirov A.N., Shikhiyeva L.M., 2024. Method for assessing the hydrate formation from a mixture of natural gas flows of varying degrees of moisture content. *Nafta-Gaz*, 80(1): 39–44. DOI: 10.18668/NG.2024.01.05.

Jennings D.W., 2005. Effects of shear and temperature on WAX Deposition Cold finger investigation with a Gulf of Mexico Crude Oil. *Energy Fuels*, 19(4): 1376–1386. DOI: 10.1021/ef049784i.

Jiang G., Tang D, Hu Q. 2018. Effect of a type of spontaneous emulsification and viscosity reduction agent on the properties of heavy oil. *Petroleum Science and Technology*, 36(10): 781–786. DOI: 10.1080/10916466.2018.1438324.

Kharisov B.I., Gonzáles M.O., Quezada T.S., de la Fuente I.G., Longoria F., 2017. Materials and nanomaterials for the removal

of heavy oil components. *Journal of Petroleum Science and Engineering*, 156: 971–987. DOI: 10.1016/j.petrol.2017.06.065.
Knapik E. 2020. Biodemulsification combined with fixed-bed biosorption for the recovery of crude oil from produced water. *Journal of Water Process Engineering*, 38: 101614. DOI: 10.1016/j.jwpe.2020.101614.
Lee J., Babadagli T. 2020. Comprehensive review on heavy-oil emulsions: Colloid science and practical applications. *Chemical Engineering Science*, 228: 115962. DOI: 10.1016/j.ces.2020.115962.
Liu D., Li C., Zhang X., Yang F., Sun G., Yao B., Zhang H. 2020. Polarity effects of asphaltene subfractions on the stability and interfacial properties of water-in-model oil emulsions. *Fuel*, 269: 117450. DOI: 10.1016/j.fuel.2020.117450.
Matiyev K.I., Agazade A.D. Keldibayeva S.S. 2016. Removal of asphalt, resin and paraffin deposits from various deposits. *SOCAR Proceedings*. 4: 64–68.
Mingalev P.G., Grishaev P.A., Ehrlich G.V., Lisichkin G.V., 2022. Magnetic sorption deasphalting of oil fractions. *Chemistry and chemistry. technology*. 11: 76–82. DOI: 10.6060/ivkkt.20226511.6700.
Nebogina N.A., Prozorova I.V., Savinykh Yu. V., Yudina N.V., 2008. The influence of natural surfactants on the stabilization of oil-water emulsions. *Petroleum Chemistry*, 50(2): 158–163. DOI: 10.1134/S0965544110020131
Roa M., Cruz-Duarte J.M., Correa R., 2021. Study of an asphaltene electrodeposition strategy for Colombian extra-heavy crude oils boosted by the simultaneous effects of an external magnetic field and ferromagnetic composites. *Fuel*, 287: 119440. DOI: 10.1016/j.fuel.2020.119440.
Roodbari N.H., Badiei A., Soleimani E., Khaniani Y., 2011. Tweens demulsification effects on heavy crude oil/water emulsion. *Arabian Journal of Chemistry*, 9: S806–S811. DOI: 10.1016/j.arabjc.2011.08.009.
Santos I.C., Oliveira P.F., Mansur C.R.E., 2017. Factors affecting crude oil viscosity and techniques to reduce it: a review. *Brazilian Journal of Petroleum and Gas*, 11: 115–130. DOI: 10.5419/BJPG2017-0010.
Shayan N.N., Mirzayi B. 2015. Adsorption and removal of asphaltene using synthesized maghemite and hematite nanoparticles. *Energy and Fuels*, 29: 1397–1406. DOI: 10.1021/ef502494d.
Taylor S. 2018. Interfacial chemistry in steam-based thermal recovery of oil sands bitumen with emphasis on steam-assisted gravity drainage and the role of chemical additives. *Colloids and Interfaces*, 20: 16. DOI: 10.3390/colloids2010016.
Wang Z., Lin X., Rui Z., Xu M., Zhan S. 2017. The Role of Shearing Energy and Interfacial Gibbs Free Energy in the Emulsification Mechanism of Waxy Crude Oil. *Energies*, 10(5): 721. DOI: 10.3390/en10050721.
Wen J., Zhang J., Wang Z., Zhang Y. 2016. Correlations between emulsification behaviors of crude oil-water systems and crude oil compositions. *Journal of Petroleum Science and Engineering*, 146: 1–9. DOI: 10.1016/j.petrol.2016.04.002.
Xia X., Ma J., Liu F., Cong H., Li X. 2023. A novel demulsifier with strong hydrogen bonding for effective breaking of water-in-heavy oil emulsions. *International Journal of Molecular Sciences*, 24(19): 14805. DOI: 10.3390/ijms241914805.
Zhang S., Liu D., Deng W., Que G. 2007. A review of slurry phase hydrocracking heavy oil technology. *Energy and Fuels*, 21(6): 3057–3066. DOI: 10.1021/ef700253f.
Zhao H., Kang W., Yang H., Huang Z., Zhou B., Sarsenbekuly B. 2021. Emulsification and stabilization mechanism of crude oil emulsion by surfactant synergistic amphiphilic polymer system. *Colloids and Surfaces A: Physicochemical and Engineering Aspects*, 609: 125726. DOI: 10.1016/j.colsurfa.2020.125726.

Legislative acts and normative documents

GOST 51858 2020 Oil. General technical conditions.
GOST 9.913-90. Laboratory test methods for corrosion properties and emulsion stability of oils and petroleum products.

Prof. Guseyn Ramazan GURBANOV, Ph.D.
Head of the Department of Oil and Gas Transportation and Storage
Azerbaijan State Oil and Industry University
16/21 Azadliq Ave., AZ1010 Baku, Azerbaijan
E-mail: *huseyn.gurbanov@asoiu.edu.az*

Aysel Valiyaddin GASIMZADE, Ph.D.
Associate Professor at the Department of Oil and Gas Transportation and Storage
Azerbaijan State Oil and Industry University
31 Khagani Street, AZ1010 Baku, Azerbaijan
E-mail: *qasimzade92@inbox.ru*